

A simple method of cartilage regeneration using a new polymerizing system: ultrastructural characteristics of the repair tissue

N. REISSIS, S. DOWNES, M. KAYSER, G. BENTLEY

The Institute of Orthopaedics and IRC in Biomedical Materials, University College, London, UK, Royal National Orthopaedic Hospital, Stanmore, Middlesex, HA7 4LP, UK

The ultrastructural characteristics of the repair tissue in large articular cartilage defects, filled with a heterocyclic polymerizing system were studied using transmission electron microscopy (TEM) and energy dispersive micro-analysis (EDMA). By six weeks post-implantation, the defects were resurfaced with predominantly hyaline-like articular cartilage. Chondrocytes in both the superficial and deep zones of the repair tissue were highly productive, secreting large amounts of proteoglycans, into a well-organized, rich in collagen fibrils, extracellular matrix. By contrast, in the repair tissue of the defects treated without the biomaterial, proteoglycan synthesis was less and the structure of the matrix was inferior. We conclude that the polymer enhances both chondrocyte metabolism and matrix organization, thus improving the quality of the repair tissue in articular cartilage defects.

1. Introduction

A new polymer system, based on poly-ethyl-methacrylate (PEMA) polymer powder and tetra-hydrofurfuryl-methacrylate (THFMA) monomer liquid, has been investigated as a potential biomaterial for articular cartilage repair. The polymer has already been shown to be well tolerated by the oral mucosa and dental pulp [1] and it has also been found, using histology and immuno-histo-chemistry that it enhances articular cartilage repair in large, full-thickness defects in the animal model [2].

The present *in vivo* study focuses on the ultrastructural characteristics of the newly formed cartilage, and provides better understanding of the mode of action of the biomaterial in articular cartilage regeneration.

2. Materials and methods

2.1. Animal model

Eight adult female Sandy-Lop rabbits were anaesthetized with 2% halothane and 3:2 mixture of nitrous oxide and oxygen. The articular cartilage defects were created by hand in the femoral trochlea of the distal femur using a 4.5 mm drill bit. One knee was operated on in each animal. The femoral trochlea articulates directly with the patella, throughout the whole range of movement of the knee joint, and it is a heavily loaded area of articular cartilage. The drill holes were washed thoroughly with normal saline to remove all osteochondral debris.

Preparation of the biomaterial was performed by mixing 1 g PEMA with 0.6 ml THFMA (containing

2.5% v/v N,N-dimethyl-p-toluidine) for 2 min at room temperature using a sterile spatula. Using a 1 ml sterile syringe, 0.1 ml of the resulting dough was injected into the osteochondral defect in four of the animals; the remaining four rabbits were used as a control. Polymerization occurred *in situ*, the top surface of the polymer plug being carefully controlled, using a specially designed instrument, to be at the level of the subchondral bone, below the level of the surrounding articular cartilage. Bleeding was carefully controlled and was minimized using hydrogen peroxide solution. Wounds were closed using absorbable sutures.

Full range of movement and full weight-bearing were allowed immediately post-operatively. The rabbits were group housed in floor pens [3] allowing maximum loading on the defect area. The rabbits were sacrificed at six weeks post-operatively by intravenous injection of pentobarbitone sodium.

2.2. Preparation for transmission electron microscopy (TEM)

The specimens were fixed in 2% glutaraldehyde in 0.1 M sodium cacodylate buffer at pH 7.2 for 24 h at 4°C, followed by secondary fixation in an aqueous solution of 1% osmium tetroxide and 1.5% potassium ferrocyanide [4–6] for 1 h. The samples were washed in the same buffer and dehydrated through a graded series of ethanols. Impregnation with a 1:1 ethanol/Spurrs' resin mixture for six hours was then carried out including two hours vacuum impregnation at

1.5×10^3 Pa. The 1:1 mixture of ethanol/Spurrs' resin was followed by four changes, 12 h each, of Spurr's resin alternating every 6 h with vacuum infiltration. The specimens were embedded and cured at 70 °C for 18 h. Sections 90 nm thick were cut on a L.K.B. Ultratome III. The sections were stained with 2% uranyl acetate and Reynold's lead citrate [7] and were picked up on 3 mm diameter copper grids. The electron microscope used was Philips CM 12, fitted with EDAX PV 9800 X-ray micro-analysis system. Unstained sections were used for the energy dispersive micro-analysis. They were probed at 80 kV with a specimen tilt of 20°, giving a final take-off angle 40°, and counted for 200 live seconds.

3. Results

The biomaterial used in this study appeared to have increased production of proteoglycans by the chondrocytes in both the superficial and the deep zone of the repair tissue. In the superficial zone chondrocytes were flat in appearance, orientated parallel to the articular surface (Fig. 1). Abundant rough endoplasmic reticulum and numerous secretory vesicles and Golgi apparatus were noted in the cells. Electron-dense granules were found around the cells and to a lesser extent throughout the matrix of the newly formed cartilage. In the control specimens by contrast, cells in the superficial zone of the repair tissue (Fig. 2) were less productive with less-developed rough endoplasmic reticulum and fewer secretory vesicles. No granules were noted around these cells or in the matrix. The latter was characteristically depleted of fibres, particularly immediately adjacent to the cells.

Throughout the deep zone of the repair tissue in the biomaterial group chondrocytes were round and large with numerous electron-dense molecules around the



Figure 1 Superficial zone of the repair tissue in the biomaterial group: flat chondrocytes with highly productive endoplasm; numerous proteoglycan molecules (electron-dense granules) can be noted around the cells and throughout the matrix (uranyl acetate and Reynold's lead citrate staining, $\times 6000$).

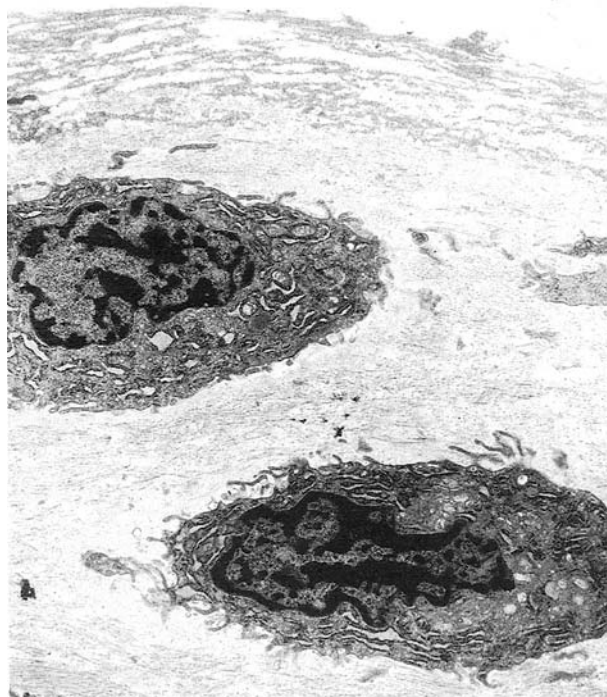


Figure 2 Superficial zone of the repair tissue in the control group: no proteoglycan molecules can be seen and the chondrocytes appear to be less productive compared to the biomaterial group (uranyl acetate and Reynold's lead citrate staining, $\times 6000$).

cells and into the surrounding matrix (Figs 3 and 4). Energy dispersive micro-analysis detected sulphur in these molecules suggesting the presence of proteoglycans (Fig. 5). In the control group no pericellular granules were noted (Fig. 6) and the matrix showed large-calibre fibrils, consistent with collagen type I, arranged in a multi-directional, disorganized fashion (Fig. 7).

Another ultrastructural characteristic observed in both groups, more common in the control group, was the formation of chondrocyte clusters (Fig. 8). They were found mainly in the deep layers of the new

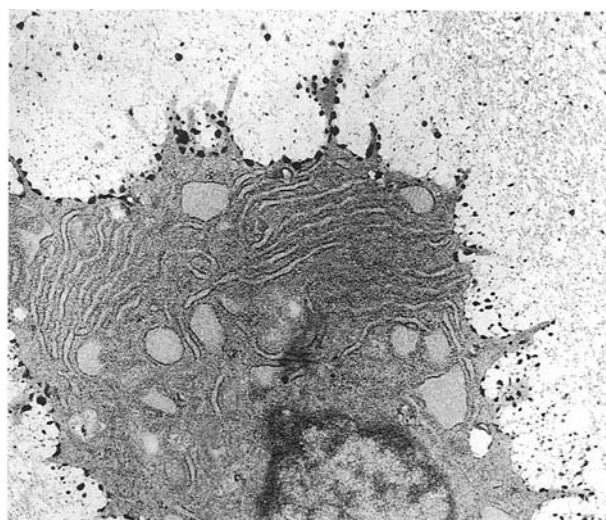


Figure 3 Deep zone of the repair tissue in the biomaterial group: large, highly productive, round chondrocytes with multiple cytoplasm processes; proteoglycan molecules (electron-dense granules) are demonstrated (uranyl acetate and Reynold's lead citrate staining, $\times 12600$).

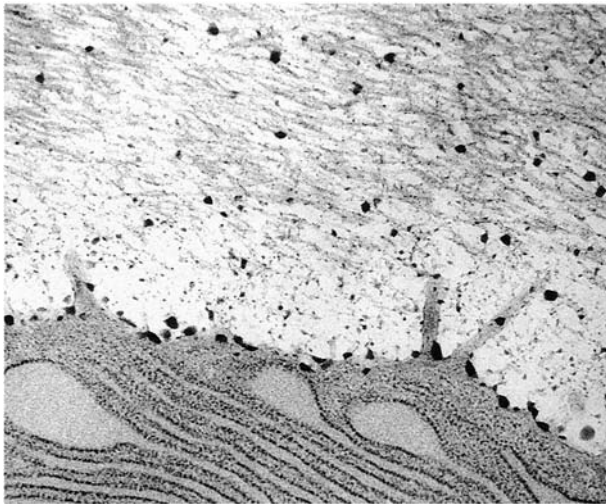


Figure 4 Deep zone of the repair tissue in the biomaterial group: higher magnification of the chondrocyte shown in Fig. 3, demonstrating proteoglycan molecules on the cell membrane and also in the extracellular matrix. The immediate pericellular matrix contains only few, small-calibre collagen fibres, compared to the rest of the extracellular matrix (uranyl acetate and Reynold's lead citrate staining, $\times 14800$).

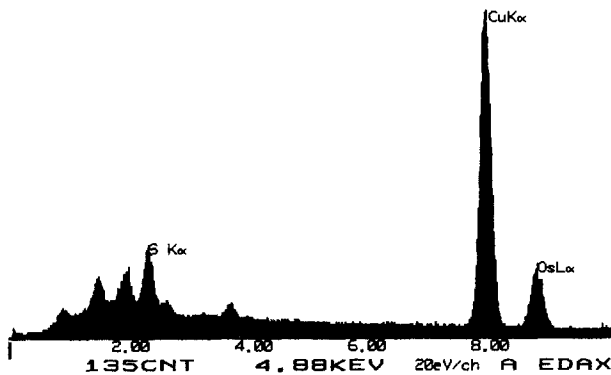


Figure 5 Energy dispersive micro-analysis: the electron-dense granules seen in Figs 3 and 4 were probed in unstained, 90 nm thick sections. Molecular sulphur ($S K_{\alpha}$ peak) was detected suggesting the presence of proteoglycans in these granules. The osmium, ($Os L_{\alpha}$ peak) is due to fixation of the specimen with osmium, while the copper ($Cu K_{\alpha}$ peak) molecule derives from the copper grid.

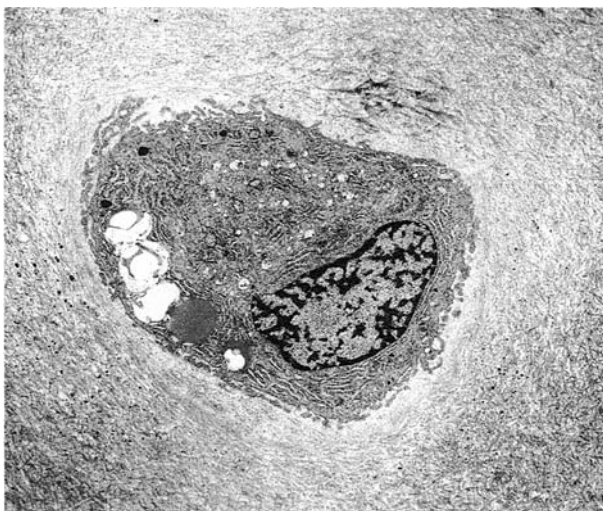


Figure 6 Deep zone of the repair tissue in the control group: lipid droplets and vacuoles were commonly seen in the cytoplasm of the chondrocytes; no proteoglycan granules could be found (uranyl acetate and Reynold's lead citrate staining, $\times 6000$).

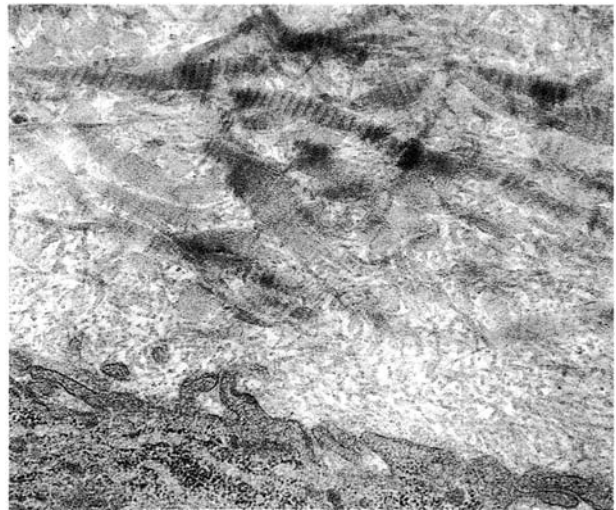


Figure 7 Deep zone of the repair tissue in the control group: higher magnification of the specimen shown in Fig. 6, demonstrating large-calibre collagen fibrils arranged in a multi-directional, disorganized fashion (uranyl acetate and Reynold's lead citrate staining, $\times 14800$).



Figure 8 Deep zone of the repair tissue in the biomaterial group: a cluster of multiple chondrocytes enclosed in a distinct pericellular capsule is demonstrated (uranyl acetate and Reynold's lead citrate staining, $\times 3200$).

cartilage, consisted of numerous chondrocytes –between 8 and 16–each one enclosed in a thin pericellular layer of small-calibre fibres. Clusters in the biomaterial group comprised of highly productive chondrocytes with large numbers of electron-dense granules around each individual cell. These granules also contained sulphur (Fig. 9). Many short processes were seen emerging from the cells within the clusters. These were significantly more numerous in the surfaces of the chondrocytes looking at the centre of the cluster rather than in those looking at its periphery (Fig. 10).

4. Discussion

In this study, a hydrophilic polymer system has been exploited in the repair of large, full-thickness articular cartilage defects in the rabbit model. It was previously

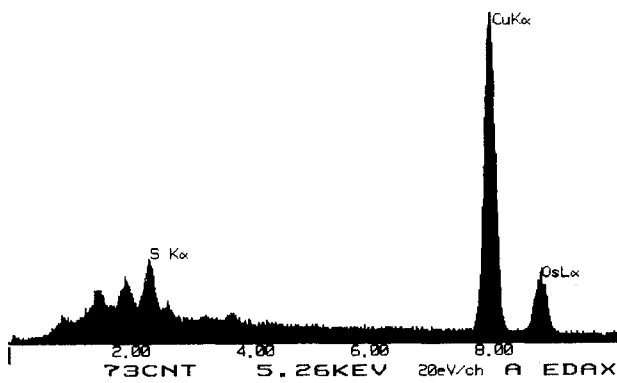


Figure 9 Energy dispersive micro-analysis: the electron-dense granules seen in Fig. 8 were probed in unstained, 90 nm thick sections. Molecular sulphur (SK_{α} peak) was detected suggesting the presence of proteoglycans in these granules, the osmium (OsL_{α} peak) is due to fixation of the specimen with osmium, while the copper (CuK_{α} peak) molecule derives from the copper grid.

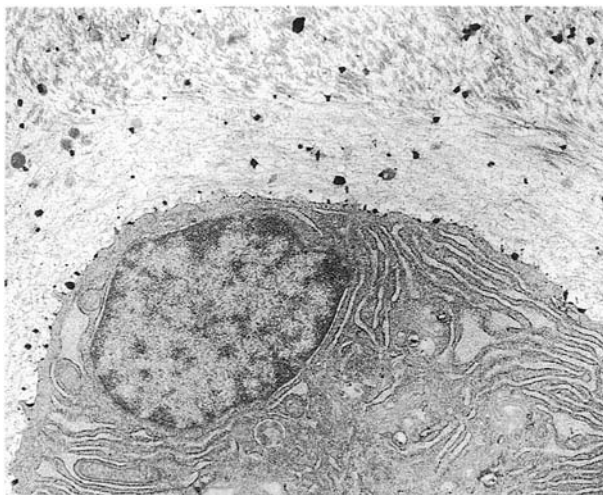


Figure 10 Deep zone of the repair tissue in the biomaterial group: higher magnification of the specimen shown in Fig. 8, focusing on the surface of the chondrocyte looking at the periphery of the cluster. Very few short cytoplasm processes can be seen. The capsule that encloses the cluster is clearly separated from the rest of the matrix of the repair tissue (uranyl acetate and Reynold's lead citrate staining, $\times 12\,600$).

shown [2] that when the top surface of the polymer plug was recessed at the level of the subchondral bone, the repair tissue consisted of hyaline-like cartilage, fully bonded to the adjacent normal articular cartilage. The present study focused on the ultrastructural characteristics of the repair tissue and showed that in the biomaterial group, chondrocytes produce significantly larger amounts of proteoglycans and also that, in the same group, organization of the collagen fibril meshwork within the matrix is superior.

It is well known that the proteoglycan content of cartilage matrix is correlated with compressive strength [8, 9] and that loss of this component leads to increased mechanical stress and subsequent dysfunction of chondrocytes [10]. Moreover, the capability of the articular cartilage to repair is related to the stress placed upon it [9] and excessive loading can be harmful. We therefore hypothesize that in the present study, the relatively larger amount of proteoglycans, secreted by the chondrocytes in the polymer group, provides a strong mechanical shelter, which prevents

cell dysfunction and death, thus improving the quality of the repair. On the other hand, it is also possible that the mal-orientation of the collagen fibrils that has mainly been recorded in the control specimens in this study, is another expression of abnormal mechanical loading on the repair area.

It has been postulated that insulin-like growth factors can be crucial for the homeostasis of the extracellular matrix of articular cartilage *in vivo* [11] and therefore it is possible that the hydrophylic bio-material used in the present experimental model attracts/adsorbs growth factors, which effectively enhance the overall repair process.

The chondron concept was introduced by Benninghoff (1925) to describe the functional and metabolic unit of the chondrocyte and its pericellular micro-environment in hyaline cartilage [12]. Ultrastructural studies have shown that the chondron in adult articular cartilage consists of a chondrocyte and its pericellular matrix, both enclosed within an impacted fibrillar capsule [13, 14]. Chondrons exist in the middle and deep layers of adult articular cartilage [13] and their pericellular matrix is rich in proteoglycans [12, 15] bound with strong crosslinks to the collagen fibril meshwork [12]. The latter consists, among other collagens, of collagen types II, VI and IX [16, 17], of which type VI collagen provides an adhesive mechanism for substratum attachment [18]. It is believed that this is exclusive to the capsule of the chondron and does not form a general component of the territorial and inter-territorial matrices [17]. As far as the function of the chondron is concerned, Poole postulates that it acts hydrodynamically to protect the chondrocyte during compressive loading [13].

In this study, clusters of multiple chondrons were noted in the repair tissue in both groups, more numerous in the control group. Each chondron in the cluster was found to be separated from the others by a layer of thin pericellular matrix, rich in small-calibre fibres. These clusters were mainly located in the deep layer of the repair tissue. We postulate that formation of clusters of multiple chondrons provides further mechanical protection against excessive/abnormal loading and, therefore, particularly in the proteoglycan depleted matrix, it help in the maintenance of the chondron's integrity and the protection of the chondrocyte during dynamic compressive loading.

We conclude that the biomaterial used in this study resulted in increased proteoglycan synthesis by the chondrocytes and in better organization of the collagen fibril meshwork in the pericellular matrix of the repair tissue. Energy dispersive micro-analysis helped in the ultra-structural characterization of the newly formed cartilage.

References

1. G. J. PEARSON, D. C. A. PICTON, M. BRADEN and C. LONGMAN, *Int. Endodontic J.* **19** (1986) 121.
2. N. REISSIS, S. DOWNES and G. BENTLEY, *Trans. Orthop. Res. Soc.* **19** (1994) 482.
3. G. R. BATCHELOR, *Animal Technol.* **42** (1991) 109.
4. W. C. DEBRUIJN, *J. Ultrastructural Res.* **42** (1973) 29.

5. A. M. DVORAK, *Lab. Investigation* **27** (1972) 561.
6. C. E. FARNUM and N. J. WILSMAN, *J. Histochem. Cytochem.* **31** (1983) 765.
7. G. ROBINSON and T. GRAY, in "Theory and practice of histological techniques" edited by J. D. Bancroft and A. Steven (Churchill Livingstone, London, 1990) p. 525.
8. J. A. BUCKWALTER, *Clin. Orthop. Rel. Res.* **172** (1983) 207.
9. C. S. CARLSON, H. D. HILLEY, C. K. HENRIKSON and D. J. MEUTEN, *Calcif. Tissue. Int.* **38** (1986) 44.
10. I. REIMANN, S. B. CHRISTENSEN and N. H. DIEMER, *Clin. Orthop. Rel. Res.* **168** (1982) 258.
11. D. J. McQUILLAN, C. J. HANDLEY, M. A. CAMPBELL, S. BOLIS, V. E. MILWAY and A. C. HERINGTON, *Biochem. J.* **240** (1986) 423.
12. C. A. POOLE, T. HONDA, S. J. M. SKINNER, J. R. SCHOFIELD, K. F. HYDE and H. SHINKAI, *Connective Tissue Res.* **24** (1990) 319.
13. C. A. POOLE, M. H. FLINT and B. W. BEAUMONT, *J. Orthop. Res.* **5** (1987) 509.
14. *Idem., ibid.* **6** (1988) 408.
15. M. T. BAYLISS, M. VENN, A. MAROUDAS and S. Y. ALI, *Biochem. J.* **209** (1983) 387.
16. C. A. POOLE, S. F. WOTTON and V. C. DUANCE, *Histochemical J.* **20** (1988) 567.
17. C. A. POOLE, S. AYAD and J. R. SCHOFIELD, *J. Cell Sci.* **90** (1988) 635.
18. T. F. LINSENMAYER, A. MENTZER, M. H. IRWIN, N. K. WALDREP and R. MAYNE, *Expl. Cell Res.* **165** (1986) 518.